

Magnetic properties of holographic multiquarks in the quark-gluon plasma

Piyabut Burikham*

*Theoretical High-Energy Physics and Cosmology Group, Department of Physics,
Faculty of Science, Chulalongkorn University, Bangkok 10330, Thailand*

November 5, 2018

Abstract

We study the magnetic properties of the coloured multiquark states in the quark-gluon plasma where the gluons are deconfined and the chiral symmetry is still broken, using the Sakai-Sugimoto model. There are two possible magnetized multiquark configurations. Both configurations converge to the same configuration at the critical field and temperature before they dissociate altogether either into less coloured multi-quarks or into other phases for a fixed density. It is also found that the multiquarks with higher colour charges respond more to the external magnetic field in both the magnetization and the degree of chiral symmetry breaking. Magnetic field also makes it more difficult for multiquark states with large colour charges to satisfy the equilibrium condition of the configuration in the gravity dual picture. As long as the chemical potential $\mu > \mu_{onset}$, the magnetized multiquarks phase is thermodynamically preferred over the magnetized vacuum. Pure pion gradient and the chiral-symmetric quark-gluon plasma (χ_S -QGP) phase for the general Sakai-Sugimoto model are discussed and compared with the multiquark phase in the presence of the magnetic field. It is found that at large densities and moderate fields, the mixed phase of multiquarks and the pion gradient is thermodynamically preferred over the χ_S -QGP.

*Email:piyabut@gmail.com, piyabut.b@chula.ac.th

1 Introduction

There has been increasing interest in the study of nuclear phase structure as well as properties of a number of nuclear phases, especially the quark-gluon plasma in the recent few years. This is due to the new perspective in the nature of strongly interacting gauge theory from the holographic principle. Motivated by the AdS/CFT correspondence [1, 2], a number of gravity models was constructed to provide shadow gauge theories which share certain essential features with the QCD in the strong coupling regime. Sakai and Sugimoto [3, 4] proposed a toy holographic model of QCD where chiral symmetry breaking can be addressed. In Sakai-Sugimoto model, gluon deconfinement and chiral symmetry restoration are two distinct phase transitions. For non-antipodal case, the chiral symmetry restoration occurs at higher temperature than the gluon deconfinement [5], therefore it is possible to have a nuclear phase where gluons are deconfined while the quarks and antiquarks could still form colour bound states.

Bergman, Lifschytz, and Lippert [6] shows that when the baryon density is sufficiently large and the temperature is not too high, gluon-deconfined phase with broken chiral symmetry accommodates a nuclear phase where baryons can exist with thermodynamical stability. Even though the baryons can exist within the phase, the quark matters containing only free quarks or antiquarks do not share the same thermodynamical stability. This can be understood as a sign of chiral symmetry breaking, the quarks prefer to be bound together by gluon exchanges in this highly-densed thermal soup. Interestingly, further investigations into whether colour multiquark states in general could exist within this nuclear phase give positive results [7].

It was suggested quite a while ago in Ref. [8] that it is possible to have $k < N$ -baryons in $\mathcal{N}_{SUSY} = 4$ background. In the gluon-deconfined phase, since free strings solution is allowed in the corresponding gravity dual theories [9], the coloured states could also exist in the plasma. Various possibilities of exotic multiquark states are studied in Ref. [10]-[13]. Colour multiquark states in the gluon-deconfined plasma are studied in Ref. [7] where $k > N$ -baryons as well as other classes of exotic multiquark states including $N + \bar{k}$ -baryons and bound state of j mesons are investigated. The phase diagram of the colour multiquarks nuclear phase, chiral-symmetric (χ S-QGP) phase, and the vacuum nuclear phase reveals that colour multiquarks are thermodynamically stable in the region where the temperature is not too high and the density is sufficiently large (Figure 8 of Ref. [7]).

In certain situations such as in the core of the neutron stars or other enormously densed astrophysical objects, exceptionally strong magnetic field is produced in addition to the high temperature and density. Under these fierce conditions, nuclear matters are pressed together so tightly that deconfinement phase transition could occur. As is shown in the phase diagram of Ref. [7], coloured multiquark states can exist in the intermediate range of temperature and sufficiently high baryon chemical potential (implying high baryon density). They are thermodynamically preferred over the other phases such as the vacuum and the chiral-symmetric deconfined phase of quark-gluon plasma (χ S-QGP). It is therefore interesting to explore magnetic properties of the nuclear phase where coloured exotic multiquarks exist under these extreme situations. It is possible that certain classes of densed stars are in

the range of temperature and density suitable for the coloured multiquarks in the gluon-deconfined soup and the magnetic properties of these states thus significantly determine their stellar structures.

Responses of the holographic nuclear matter to the external magnetic field have been intensively investigated in Ref. [14]-[19]. It was found in Ref. [14] that the external magnetic field makes gluon-deconfined vacuum more stable thermodynamically than the case when there is no magnetic field, *i.e.* the transition temperature into the chiral-symmetric quark-gluon plasma increases with the magnetic field and saturates in the limit of an infinite field. Authors of Ref. [19] found a phase transition induced by the external magnetic field in the χ S-QGP phase. This could be traced back to the nonlinearity of the DBI action used to describe the holographic nuclear matter. Since this transition occurs when the magnetic field changes from small to large strength, the Yang-Mills approximation approach [17] is no longer valid and similar transition is not found without consideration of the full DBI action. We take the full DBI approach and investigate the magnetic responses of the multiquark nuclear phase with broken chiral symmetry in this article. We found that the magnetized multiquarks phase are always thermodynamically preferred over the magnetized vacuum. At a fixed density, it is also found that the multiquark states can satisfy the scale fixing condition up to certain critical values beyond which they would change into multiquarks with smaller colour charges. For higher magnetic fields, all of the multiquarks cannot satisfy the scale fixing condition at the same density and we would expect other phases to set in or the density has to be increased for the multiquark configuration to be able to satisfy the scale fixing condition.

There are two multiquark configurations found below a critical field. The two configurations merge into one at the critical field and temperature for a fixed density. By comparing to the pure pion gradient and the χ S-QGP phase, the multiquark phase is found to be preferred thermodynamically at large densities and moderate fields.

In Sec. 2, the essential features of the multiquarks are reviewed. Magnetic responses and relevant magnetic phases of the colour multiquarks are studied in Sec. 3 using the DBI action. Comparison to the pure pion gradient and the χ S-QGP phase is discussed in Sec. 4. We discuss the results and make some conclusions in Sec. 5.

2 Exotic multiquark states in the Sakai-Sugimoto model

In the Sakai-Sugimoto model, gluon deconfinement and the chiral-symmetry restoration are two distinct phase transitions. Generically they occur at different temperatures. When the gluons become deconfined at the deconfinement phase transition, quarks could still be bound together by the free gluons due to the fact that the coupling is still strong (provided that the density is sufficiently high) and therefore the chiral symmetry could still be broken. Due to the deconfinement, the bound states of multiquarks are not colour singlet in general. Certain properties of the coloured multiquarks are studied in Ref. [7] where it is demonstrated that the coloured states could exist with thermodynamical stability. When the temperature rises further, the bound states become less and less stable and finally completely dissolved into the

quark-gluon plasma. The chiral symmetry is restored and everything becomes completely deconfined.

It was proposed by Witten [20], Gross and Ooguri [21] that a D-brane wrapping internal subspace of a holographic background could describe a colour-singlet bound state of N quarks in the dual $U(N)$ gauge theory. A wrapping D-brane sources $U(1)$ gauge field on its world volume and induces an N units of $U(1)$ charge upon itself. This charge needs to be cancelled by N external strings connecting to the wrapping brane. The wrapping brane with N strings attached is called a baryon vertex.

In the gluon-deconfined phase, more strings can be attached to the baryon vertex provided that there are equal number of strings stretching out and go to the background horizon. This configuration still conserves the $U(1)$ charge of the brane and solve the equation of motion of the Nambu-Goto action [9]. We can parameterize the number of radial strings stretching from the vertex to the horizon as k_r and the number of strings connecting the vertex to the boundary of the background as k_h . For the $k > N$ -baryon, $k_h - k_r = N$ whilst for $k < N$ -baryon, $k_h + k_r = N$. Other classes of exotic multiquark states can be constructed by adding more strings in and out of the vertex. Few examples are given in Ref. [7] where some interesting properties are also discussed.

There could exist an interaction among the multiquarks in the form of connecting strings between each vertex very similar to the string connecting two end points of quark and anti-quark in the holographic meson configuration. A multiquark can use one of the radial strings to merge with another radial string from neighbouring multiquark and form a colour binding interaction (while keeping k_h fixed). Therefore the number of radial strings represents the *colour charges* of the multiquark. When the gluons are deconfined, the “direct” colour interaction would be approximately the same as the meson and baryon binding potential of the Coulomb type plus some screening effect. Neglecting the direct interaction and considering only the DBI-induced collective behaviour of the gas of multiquarks [6, 7], an approximate phase diagram can be obtained showing exotic nuclear phase where multiquarks can exist with thermodynamic stability. Schematic configurations of the three gluon-deconfined phases are given in Fig. 1 where the direction along the circle is the compactified coordinate x_4 and the vertical direction is the radial coordinate u .

3 Magnetic properties of the coloured multiquarks in the nuclear phase

The setup we use is the Sakai-Sugimoto (SS) model with the source terms from the instanton embedded in the $D8 - \overline{D8}$ configuration, and the radial strings similar to the configuration used in Ref. [7]. The instanton (the baryon vertex being pulled up all the way to the position of the D8-branes by the strings connecting between the vertex and the flavour branes) is embedded within the D8-branes and acts as a source for the baryon density, d . The radial strings stretching from the instanton down to the horizon of the background act as another source. The number of radial strings is parameterized by $n_s = (\text{number of radial strings})/N$. It also tells us how much colour charges a multiquark has.

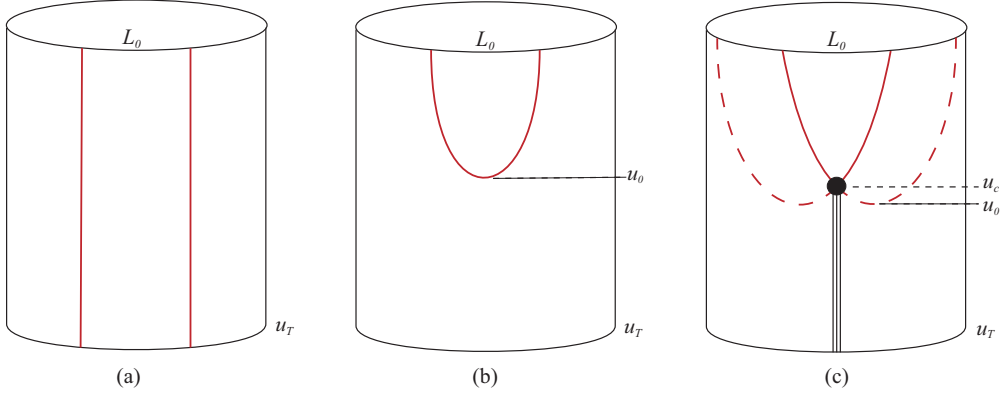


Figure 1: Configurations of χ S-QGP (separate D8, $\overline{\text{D8}}$)(a), vacuum (merging D8 and $\overline{\text{D8}}$)(b) and exotic nuclear phase (vertex attached to the D8- $\overline{\text{D8}}$ with radial strings stretch down to horizon)(c).

The baryon chemical potential is also generated on the D8-branes by the vector part, a_0^V , of the $U(1)$ subgroup of the $U(n_f)$ flavour group of the D8-branes. The magnetic field is then turned on by another part of the $U(1)$. We choose the direction of the magnetic field so that the vector potential is

$$a_3^V = Bx_2. \quad (1)$$

The vector part a_0^V is related to the baryon chemical potential μ by

$$\begin{aligned} \mu &= a_0^V(u \rightarrow \infty), \\ a_0^V(u_c) &= \mu_{source}, \\ \mu_{source} &= \frac{1}{\mathcal{N}} \frac{\partial S_{source}}{\partial d}. \end{aligned} \quad (2)$$

The contributions from the sources, μ_{source} , are from the baryon vertex and the radial strings. The full expressions are given in the Appendix. The contribution from the $U(1)$ vector gauge field in the D8-branes, μ , corresponds to the baryon chemical potential from the content of the plasma. The five-dimensional Chern-Simon term of the D8-branes generates another axial part of the $U(1)$, a_1^A , by coupling it with B and a_0^V . In this way, the external magnetic field induces the axial current j_A associated with the axial field a_1^A .

The background metric of the Sakai-Sugimoto model is

$$ds^2 = \left(\frac{u}{R_{D4}} \right)^{3/2} (f(u)dt^2 + \delta_{ij}dx^i dx^j + dx_4^2) + \left(\frac{R_{D4}}{u} \right)^{3/2} \left(u^2 d\Omega_4^2 + \frac{du^2}{f(u)} \right)$$

$$F_{(4)} = \frac{2\pi N}{V_4} \epsilon_4, \quad e^\phi = g_s \left(\frac{u}{R_{D4}} \right)^{3/4}, \quad R_{D4}^3 \equiv \pi g_s N l_s^3,$$

where $f(u) \equiv 1 - u_T^3/u^3$, $u_T = 16\pi^2 R_{D4}^3 T^2/9$. The volume of the unit four-sphere Ω_4 is denoted by V_4 and the corresponding volume 4-form by ϵ_4 . l_s and g_s are the string length

scale and the string coupling. The x_4 coordinate is compactified with radius R which is generically different from the curvature R_{D4} of the background.

The DBI and the Chern-Simon actions of the D8-branes in this background can be computed to be

$$S_{D8} = \mathcal{N} \int_{u_c}^{\infty} du u^{5/2} \sqrt{1 + \frac{B^2}{u^3}} \sqrt{1 + f(u)(a_1^A)^2 - (a_0^V)^2 + f(u)u^3 x_4'^2} \quad (3)$$

$$S_{CS} = -\frac{3}{2} \mathcal{N} \int_{u_c}^{\infty} du (\partial_2 a_3^V a_0^V a_1^A - \partial_2 a_3^V a_0^V a_1^A). \quad (4)$$

The normalization factor, $\mathcal{N} = NR_{D4}^2/(6\pi^2(2\pi\alpha')^3)$, represents the brane tension. The explanation of the factor $3/2$ is given in Ref. [16] where it could be understood as representing the edge effect of the finite region with uniform magnetic field. The equations of motion with respect to a_0^V, a_1^A are

$$\frac{\sqrt{u^5 + B^2 u^2} f(u) a_1^A}{\sqrt{1 + f(u)(a_1^A)^2 - (a_0^V)^2 + f(u)u^3 x_4'^2}} = j_A - \frac{3}{2} B\mu + 3Ba_0^V, \quad (5)$$

$$\frac{\sqrt{u^5 + B^2 u^2} a_0^V}{\sqrt{1 + f(u)(a_1^A)^2 - (a_0^V)^2 + f(u)u^3 x_4'^2}} = d - \frac{3}{2} Ba_1^A(\infty) + 3Ba_1^A. \quad (6)$$

The quantities d, j_A are the corresponding density and current density at the boundary of the background ($u \rightarrow \infty$), they are defined to be

$$j^\mu(x, u \rightarrow \infty) = \frac{\delta S_{eom}}{\delta A_\mu} \Big|_{u \rightarrow \infty} \quad (7)$$

$$= (d, \vec{j}_A). \quad (8)$$

Explicitly, they are

$$d = \frac{\sqrt{u^5 + B^2 u^2} a_0^V}{\sqrt{1 + f(u)(a_1^A)^2 - (a_0^V)^2 + f(u)u^3 x_4'^2}} \Big|_{\infty} - \frac{3}{2} Ba_1^A(\infty), \quad (9)$$

$$j_A = \frac{\sqrt{u^5 + B^2 u^2} f(u) a_1^A}{\sqrt{1 + f(u)(a_1^A)^2 - (a_0^V)^2 + f(u)u^3 x_4'^2}} \Big|_{\infty} - \frac{3}{2} B\mu. \quad (10)$$

For our multiquark configuration, the D8-branes starts from $\bar{u} = u_c$ and extends to $u \rightarrow \infty$. At the boundary ($u \rightarrow \infty$), the chiral symmetry is broken and therefore the value of $a_1^A(\infty)$ is taken to be a physical field, $\nabla\varphi$ [16], describing the degree of chiral symmetry breaking. The total action is minimized with respect to $a_1^A(\infty)$ if the axial current j_A (also defined at the boundary) is zero.

The total action does not depend on $x_4(u)$ explicitly, therefore the constant of motion leads to

$$(x_4'(u))^2 = \frac{1}{u^3 f(u)} \left[\frac{u^3 [f(u)(C(u) + D(u)^2) - (j_A - \frac{3}{2} B\mu + 3Ba_0^V)^2]}{F^2} - 1 \right]^{-1}, \quad (11)$$

where

$$F = \frac{u_c^3 \sqrt{f(u_c)} \sqrt{f(u_c)(C(u_c) + D(u_c)^2) - (j_A - \frac{3}{2}B\mu + 3Ba_0^V(u_c))^2} x_4'(u_c)}{\sqrt{1 + f(u_c)u_c^3 x_4'^2(u_c)}} \quad (12)$$

and $C(u) \equiv u^5 + B^2u^2$, $D(u) \equiv d + 3Ba_1^A(u) - 3B\nabla\varphi/2$. The expression of $x_4'(u_c)$ is given in the Appendix. It is determined from the force condition and the scale fixing condition

$$L_0 = 2 \int_{u_c}^{\infty} x_4'(u) du = 1. \quad (13)$$

Since $x_4'(u)$ depends on both $a_0^V(u)$, $a_1^A(u)$, we need to solve the differential equations (5) and (6) with $x_4'(u)$ substituted into the equations of motion and check whether the solutions satisfy the scale fixing condition Eqn. (13). The values of the vector and axial field at the vertex are also chosen so that $a_0^V(u_c) = \mu_{source}$, $a_1^A(u_c) = 0$. We basically perform the shooting algorithm by choosing the value of μ and $\nabla\varphi$ in the expression for $x_4'(u_c)$ until we hit $a_0^V(\infty) = \mu$ and $a_1^A(\infty) = \nabla\varphi$. If the resulted solution satisfies the scale fixing condition $L_0 = 1$, we keep the solution. If not, we adjust the value of u_c and perform the shooting procedure again. The position u_c for $n_s = 0$ is given as a function of the density, the magnetic field, and the temperature in Fig. 2.

From the solutions of the equations of motion, the relations between baryon chemical potential (μ) and the baryon density (d), the magnetic field (B), and the temperature (T) are obtained for the choice of parameters $n_s = 0$ (normal baryon), $j_A = 0$, as are shown in Figure 3. There are two types of solution corresponding to the two holographic multiquark configurations. One is the configuration with u_c close to u_T (configuration-**A**) and another is the configuration with a large separation between u_c and u_T (configuration-**B**).

The baryon chemical potential is found to be an increasing function of the density for most range of d for both configuration **A**, **B**. As is shown in Fig. 2, configuration-**A** has the position of vertex u_c closer to the horizon u_T than configuration-**B**. At very small d , the two configurations emerge separately as two distinct configurations. Interestingly, as the magnetic field and temperature increase, the two configurations converge into a single configuration as we can see the position u_c approaches the same value at the critical field and temperature (see Fig. 2). However, when the two configurations merge, the configuration no longer satisfies the scale fixing condition $L_0 = 1$ and we expect it to change into other phases such as the chiral-symmetric quark-gluon plasma for a fixed density. It turns out that if the density is allowed to change, the multiquark configuration can continue to satisfy the scale fixing condition at higher fields provided that the density is sufficiently large. This will be discussed more in Section 4.

In Fig. 3, the baryon chemical potential is an increasing function of d , this is true for both configuration-**A** and **B**. It is roughly a linear function of the density, showing that the DBI-induced collective interaction between the multiquarks are negligible. As d gets larger, the DBI-induced effect sets in and the negative binding interaction makes μ grows with d less quickly than the linear progression. Note that this DBI-induced interaction occurs even when the baryon is colour singlet due to the nonlinear nature of the DBI action. The origin

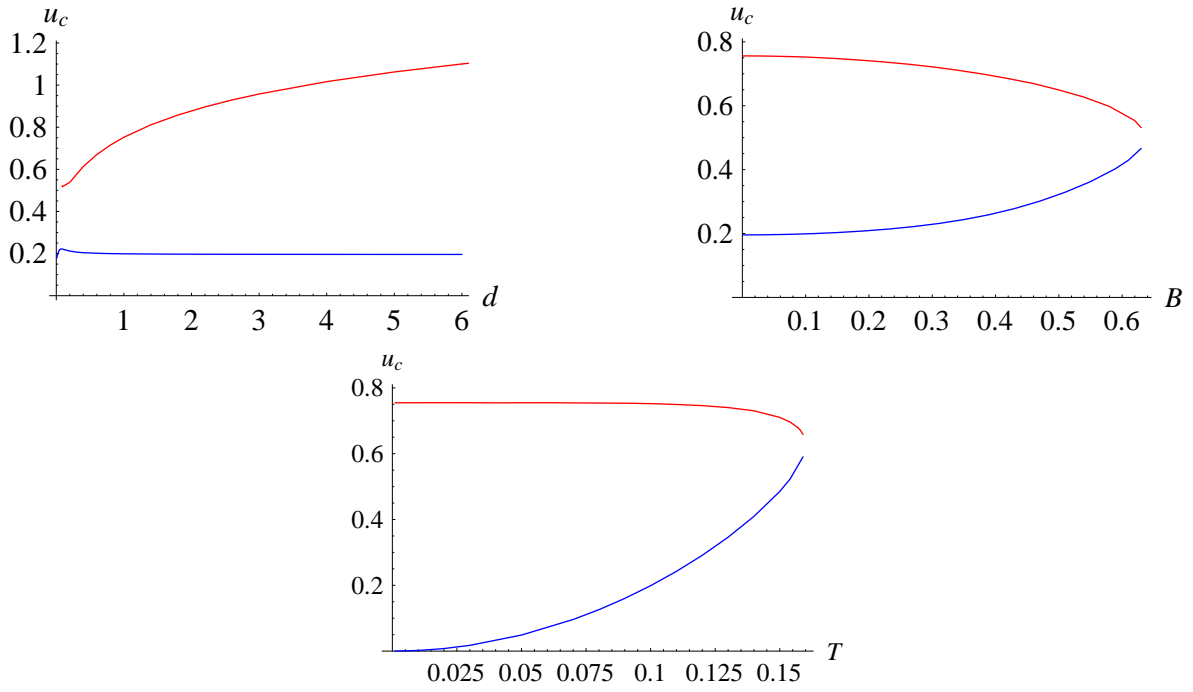


Figure 2: Position u_c of the vertex for $n_s = 0$ (normal baryon) and fixed $j_A = 0$ as a function of (a) d with fixed $B = 0.10, T = 0.10$, (b) B with fixed $d = 1, T = 0.10$, (c) T with fixed $B = 0.10, d = 1$. The lower (blue) line is the configuration-**A** with u_c close to u_T and the upper (red) line is the configuration-**B** with large separation between u_c and u_T .

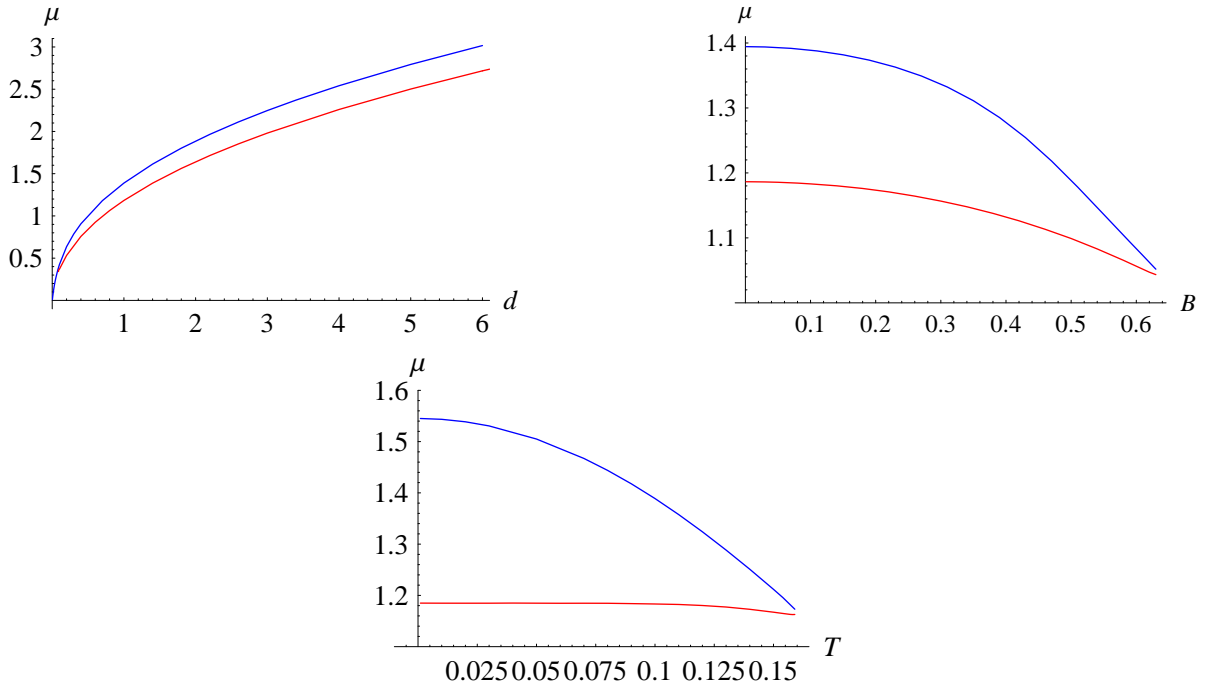


Figure 3: The baryon chemical potential μ for $n_s = 0$ (normal baryon) and fixed $j_A = 0$ as a function of (a) d with fixed $B = 0.10, T = 0.10$, (b) B with fixed $d = 1, T = 0.10$, (c) T with fixed $B = 0.10, d = 1$. The upper (blue) line is the configuration-**A** with u_c close to u_T and the lower (red) line is the configuration-**B** with large separation between u_c and u_T .

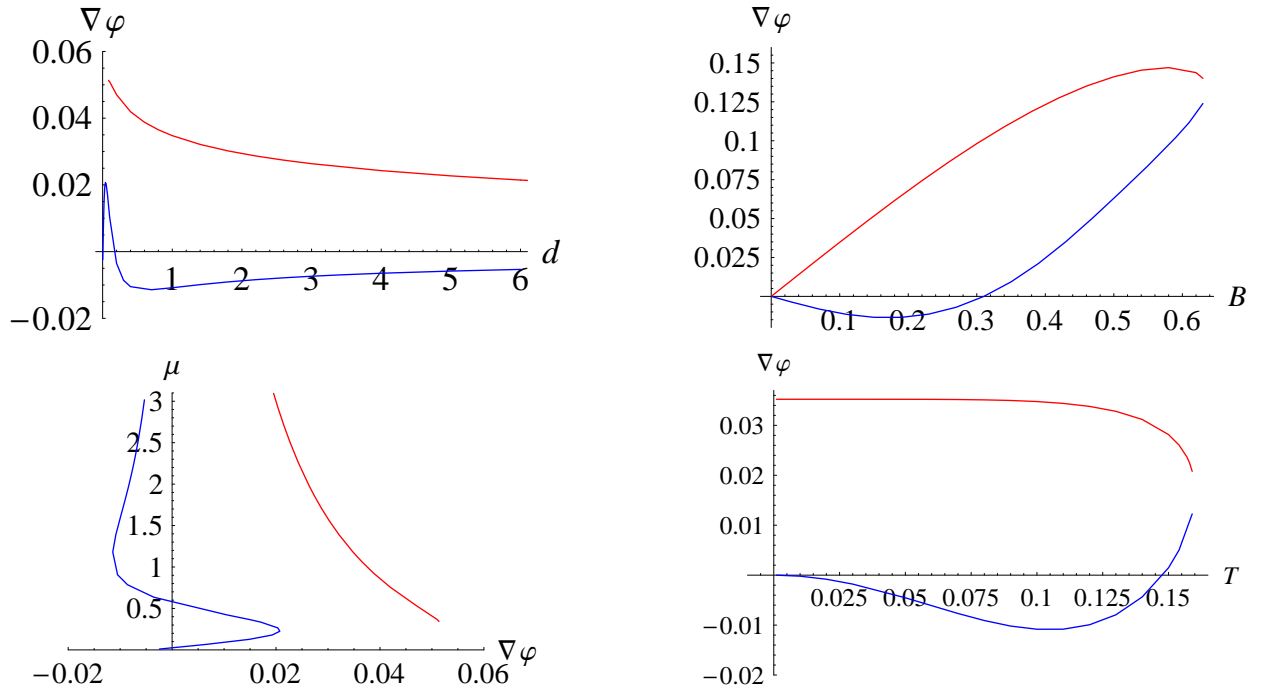


Figure 4: The gradient of the scalar field $\nabla\varphi \equiv a_1^A(\infty)$ for $n_s = 0$ (normal baryon) and fixed $j_A = 0$ as a function of (a) d with fixed $B = 0.10, T = 0.10$, (b) B with fixed $d = 1, T = 0.10$, (c) μ with fixed $B = 0.10, T = 0.10$, (d) T with fixed $B = 0.10, d = 1$. The lower (blue) line is the configuration-**A** with u_c close to u_T and the upper (red) line is the configuration-**B** with large separation between u_c and u_T .

of this DBI-induced interaction is the “*tidal weight*” of the DBI action contributed from both the branes’ worldsheet metric and the background gauge field strength. Naturally, any form of energy contributes to the tidal weight even the colour singlets.

For configuration-**B**, there seems to be minimal density d_{min} below which the shooting algorithm could not find other valid solutions. We are not certain what happens below these values. It is possible that when the field is turned on, the D8-branes acquire higher tension and therefore the configuration requires minimal density to pull it down in order for the distance between D8 and $\overline{\text{D8}}$ to reach $L_0 = 1$. For $T = 0.10, B = 0.10, n_s = 0$, the value of d_{min} for multiquark configuration **B** is approximately 0.086.

Figure 3 shows that the chemical potential is a decreasing function with respect to the magnetic field. This is similar to the behaviour of baryons in chiral-symmetric quark-gluon plasma studied in Ref. [16]. When the field gets stronger up to certain values, the field becomes too strong for the force condition to hold at the scale fixing $L_0 = 1$. This strange behaviour is shown in Fig. 6 where multiquarks with smaller n_s are shown to be able to exist up to stronger fields.

As is also shown in Fig. 3, the relationship between μ and T is as we expect, a decreasing function of T for fixed density d since higher temperature will melt the multiquarks away. For fixed d and B , the multiquark configuration satisfies the scale fixing condition up to a maximum temperature above which we expect it to melt into the plasma. For $n_s = 0$, this critical temperature is about 0.159 for $d = 1$.

It is interesting to note that the baryon chemical potential of $n_s = 0$ multiquarks for both configurations converge to the same value at critical field ($\simeq 0.63$) and temperature ($\simeq 0.159$) for $d = 1$. This behaviour also shows up in the gradient scalar field as is shown in Fig. 4.

Fig. 4 shows the relations between the field $\nabla\varphi$ and the density, the magnetic field, the baryon chemical potential, and the temperature. The pion gradient $\nabla\varphi$ represents the domain wall of the scalar field induced by the magnetic field on the nuclear vacuum [22]. Roughly speaking, it quantifies the degree of chiral symmetry breaking. The domain wall carries baryon charge and thus contributes to the baryon density. For multiquark configuration-**B**, it increases with B for a fixed density. From Fig. 4, the pion gradient field increases linearly with respect to the field for small fields. Then it starts to saturate closed to the critical field. This is somewhat similar to the behaviour of the pion gradient in the confined phase studied in Ref. [16]. For configuration-**B**, the pion gradient field is a decreasing function of the density when the field is fixed. This implies that for a fixed magnetic field, the population of the domain wall becomes lesser as the density of the baryon (including multiquarks and other bound states) increases. We will see this behaviour again in Sect. 4 when we consider the pure pion gradient phase. Finally from Fig. 4, the degree of chiral symmetry breaking $\nabla\varphi$ decreases as temperature rises for multiquark configuration-**B**.

For configuration-**A**, the pion gradient field decreases at first for small magnetic fields, but turns to rise with the field around $B \approx 0.16$ until it converges to configuration-**B** at the critical field. The dependence of the field $\nabla\varphi$ on the density at a fixed $B = 0.10, T = 0.10$ shows a minimum at $d \approx 0.7$, corresponding to $\mu \approx 1.18$. Then as the density grows, the pion gradient increases and saturates, implying limited contribution of the domain wall for large baryon density. The temperature dependence of the pion gradient field for multiquark

configuration-**A** shows some peculiar behaviour. First, it becomes more negative at low temperatures then turns to rise and converge to configuration-**B** at the critical temperature.

Figure 7 shows how the pion gradient field $\nabla\varphi$ varies with the magnetic field B for $n_s = 0, 0.10, 0.20$. For the same B , multiquarks with higher n_s responds more to the magnetic field by inducing larger $\nabla\varphi$, implying higher degree of chiral symmetry breaking. The pion gradient field for both multiquark configuration-**A**,**B** forms a butterfly-wing shape graph for each n_s . The edge of the wing is at the critical field where the configuration converges and barely satisfies the scale fixing condition.

The magnetization of the multiquarks nuclear matter can be defined using the regulated free energy, $\mathcal{F}_E = \Omega(\mu, B) + \mu d$, in the canonical ensemble as

$$M(d, B) = -\left.\frac{\partial\mathcal{F}_E(d, B)}{\partial B}\right|_d, \quad (14)$$

where $\Omega(\mu, B) = S[a_0(u), a_1(u)](e.o.m.) - S[\text{magnetized vacuum}]$. The action with a_0^V, a_1^A eliminated is given by $S[a_0(u), a_1(u)](e.o.m.) = S_{D8} + S_{CS}$ where

$$S_{D8} = \mathcal{N} \int_{u_c}^{\infty} du C(u) \sqrt{\frac{f(u)(1 + f(u)u^3x_4'^2)}{f(u)(C(u) + D(u)^2) - (j_A - \frac{3}{2}B\mu + 3Ba_0^V)^2}},$$

and S_{CS} is given in the Appendix. The grand canonical potential is regulated with respect to the magnetized vacuum. The action of the magnetized vacuum with non-vanishing x_4' is

$$S[\text{magnetized vacuum}] = \int_{u_0}^{\infty} \left.\sqrt{C(u)(1 + f(u)u^3x_4'^2)}\right|_{vac} du,$$

where

$$x_4'(u)|_{vac} = \frac{1}{\sqrt{f(u)u^3\left(\frac{f(u)u^3C(u)}{f(u_0)u_0^3C(u_0)} - 1\right)}}. \quad (15)$$

The position u_0 where $x_4'(u_0) = \infty$ of the magnetized vacuum can be solved numerically from $L_0 = 1$ (with u_0 replacing u_c in the limit of integration). The relation between u_0 and the magnetic field is shown in Fig. 5 for $T = 0.10$. As the magnetic field gets stronger, the position of the lowest position of the D8- $\overline{\text{D8}}$ configuration, u_0 , becomes larger, in order to satisfy the condition $L_0 = 1$ (implying heavier branes due to magnetic field energy). At $T = 0.10$, position of u_0 saturates to the value of about 1.23 (The number changes with temperature, of course) in the limit of an infinite field.

The magnetization of the multiquark nuclear matter is shown in Fig. 8 for $n_s = 0$ (red), 0.10 (green), 0.20 (blue). The magnetization is positive and increases as B increases until the field is close to the critical value then it starts to drop. Generically, configuration-**A** of multiquarks has larger magnetization than configuration-**B**. For the configuration-**B** (**A**), multiquarks with higher (lower) n_s have higher magnetizations. As the magnetic field gets stronger beyond the critical field for each n_s , the multiquarks will undergo a transition into

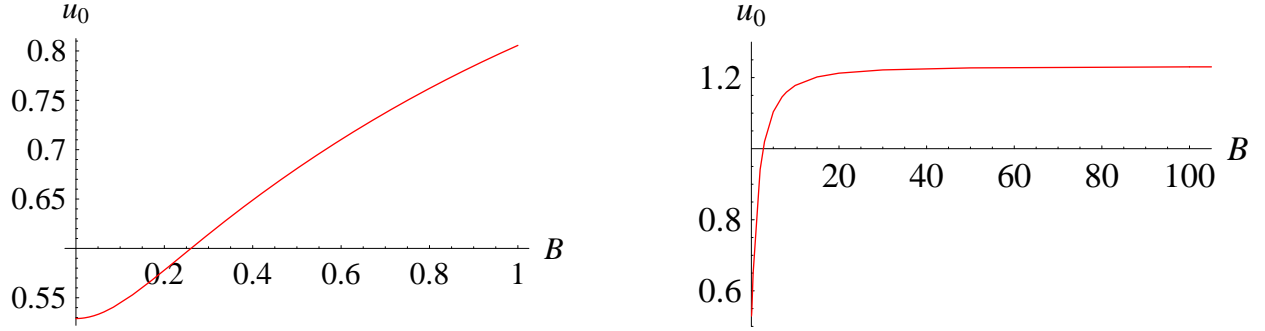


Figure 5: Relation between u_0 and external magnetic field B of the vacuum for the temperature $T = 0.10$, u_0 saturates to the approximate value of 1.23 at large field.

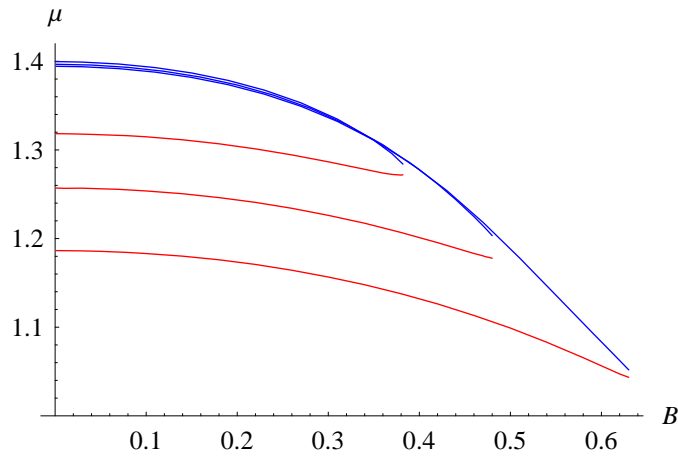


Figure 6: Comparison between the baryon chemical potential as a function of B at fixed $j_A = 0, d = 1, T = 0.10$ and (a) $n_s = 0$ (normal baryon), the bottom graph, (b) $n_s = 0.10$, the middle graph, (c) $n_s = 0.20$, the top graph. The upper (blue) lines are the configuration-**A** with u_c close to u_T and the lower (red) lines are the configuration-**B** with large separation between u_c and u_T .

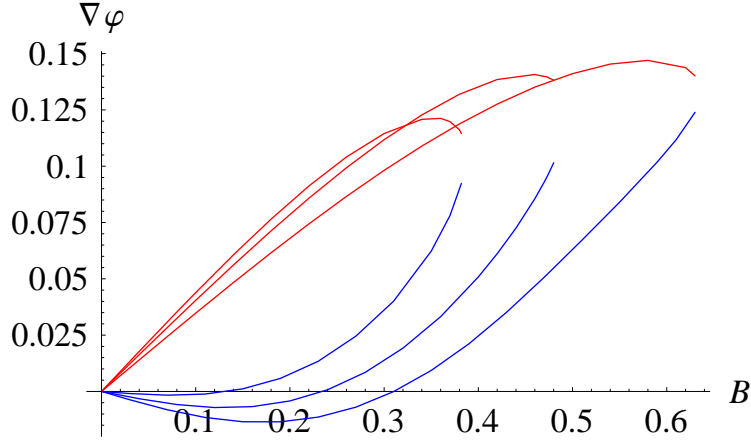


Figure 7: Comparison between the gradient of the scalar field $\nabla\varphi$ as a function of B at fixed $j_A = 0, d = 1, T = 0.10$ and (a) $n_s = 0$ (normal baryon), the bottom graph, (b) $n_s = 0.10$, the middle graph, (c) $n_s = 0.20$, the top graph. The lower (blue) lines are the configuration-**A** with u_c close to u_T and the upper (red) lines are the configuration-**B** with large separation between u_c and u_T .

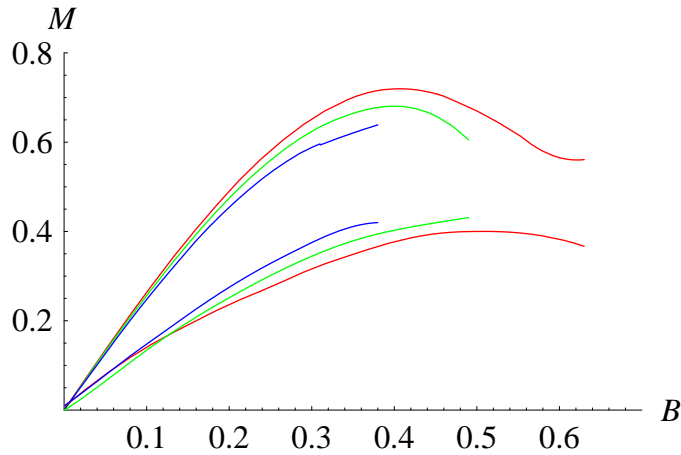


Figure 8: The magnetization of the multi-quarks nuclear matter at fixed $j_A = 0, d = 1$, and $T = 0.10$ for $n_s = 0$ (red), 0.10 (green), 0.20 (blue). The upper lines are the configuration-**A** with u_c close to u_T and the lower lines are the configuration-**B** with large separation between u_c and u_T .

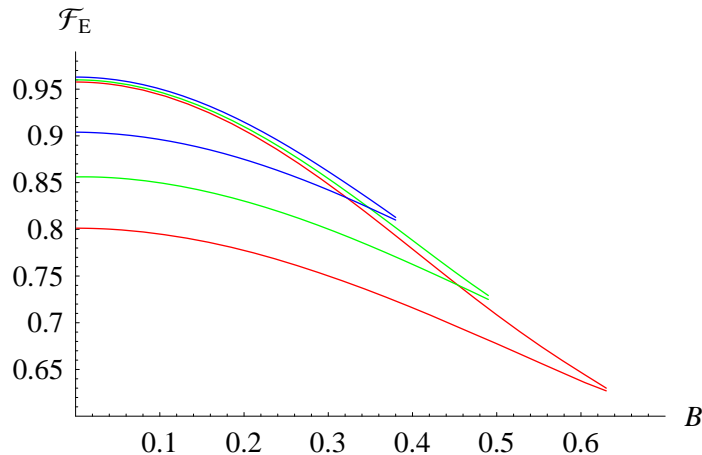


Figure 9: The free energy of the multiquarks nuclear matter at fixed $j_A = 0, d = 1$, and $T = 0.10$ for $n_s = 0$ (red), 0.10 (green), 0.20 (blue). The upper lines are the configuration-**A** with u_c close to u_T and the lower lines are the configuration-**B** with large separation between u_c and u_T .

the ones with smaller n_s . For even larger fields, even the $n_s = 0$ multiquarks cannot satisfy the scale fixing condition if the density is not allowed to change.

Interestingly, numerical studies reveal that the grand canonical potential of the multi-quark phase is always lower than the grand canonical potential of the magnetized vacuum, i.e. $S[a_0(u), a_1(u)](e.o.m.) - S[\text{magnetized vacuum}] < 0$, for the entire range of B . This suggests that once $\mu > \mu_{onset}$, the magnetized multiquark phase is always thermodynamically preferred over the magnetized vacuum, the situation similar to the case when there is no magnetic field investigated in Ref. [7]. Among the two configurations, we found from Fig. 9 that the free energy of configuration-**B** is always lower than configuration-**A** and thus more stable thermodynamically. These two multiquark configurations-**A**,**B** are the long and short cusp configurations discussed in Ref. [6], being extended to the general case with nonzero magnetic fields. It is found here that for a fixed density, strong field and/or high temperature (see Fig. 3 and 4) converge the two into a single configuration right before dissociating them altogether.

Figure 9 shows how the free energy changes with the magnetic field for $n_s = 0$ (red), 0.10 (green), 0.20 (blue) at the temperature $T = 0.10$ and the density $d = 1$. For each n_s , both configurations converge to the same configuration (with the same baryon chemical potential, degree of chiral symmetry breaking and free energy) at the critical fields. The critical fields for $n_s = 0, 0.1, 0.2$ are roughly 0.63, 0.48, 0.38 respectively.

4 Comparison to other phases

In this section we compare the baryon chemical potential and free energy of the magnetized multiquarks to the pure pion gradient phase and the chiral symmetric quark-gluon

plasma (χ_S -QGP) phase, both under the external magnetic field with gluons deconfined. The pure pion gradient phase is defined to be the phase with $\mu_{source} = 0$ (sourceless case) and the baryon chemical potential comes purely from the induced gradient field, $\nabla\varphi$, in response to the external field. The baryon density also comes purely from the pion gradient field ($d = 3B\nabla\varphi/2$). A similar situation in the confined phase of the antipodal SS model has been studied in Ref. [16]. The χ_S -QGP under the presence of the external magnetic field has been explored in Ref. [16, 19] but again only limited to the antipodal case of the SS model. In this section we explore some of their magnetic properties in more general case where $x'_4(u)$ is not zero and the scale is fixed to $L_0 = 1$. Even though the extra constraints are irrelevant to the χ_S -QGP (since $x'_4 = 0$ for this configuration), it makes crucial difference in the case of pure pion gradient phase. The scale fixing condition is found to be very difficult for the pure pion gradient configuration to satisfy for most of the density as we will discuss below.

All three phases under consideration obey the same set of equations of motion, Eqn. (5),(6) with each specific set of the boundary conditions and parameters as the following,

multiquark phase: $j_A = 0, \mu_{source} = a_0^V(u_c), \nabla\varphi = a_1^A(\infty), a_1^A(u_c) = 0,$

pure pion gradient phase: all the same with the multiquark phase with the following exceptions, $\mu_{source} = 0, a_0^V(u_c) \neq 0, d = \frac{3}{2}B\nabla\varphi,$

χ_S -QGP: $x'_4(u) = 0$ and $\nabla\varphi = a_1^A(\infty) = 0, \mu_{source} = a_0^V(u_c = u_T) = 0, j_A = \frac{3}{2}B\mu$ (since the configuration extends to u_T and $f(u_T) = 0$ so that Eqn. (5) is zero).

First, we will explore certain properties of the pure pion gradient phase and show that it does not exist in the range of parameters ($d \geq 1, B \leq 1 - 2$) under consideration. Then comparison between the multiquark and the χ_S -QGP phases will be discussed.

4.1 Pure pion gradient phase

For pure pion gradient configuration, the contribution of the sources, the vertex and strings, is set to zero.. Effectively, we set $\mu_{source} = 0, d = 3B\nabla\varphi/2$. This is because when $\nabla\varphi$ is zero, the density d should represent the density of the sources, i.e. the pure multiquark or pure baryon configuration, therefore the source density should be given by $d - \frac{3}{2}B\nabla\varphi$ on the right-hand side of Eqn. (6). When we fix the value of the density at a fixed magnetic field, $\nabla\varphi$ is also fixed. For example, when $d = 1, B = 0.1, \nabla\varphi \simeq 6.667$, a relatively large value. This large value of $\nabla\varphi = a_1^A(\infty)$ leads to a generically large value of $a_1^A(u)$ for the most range of u . From Eqn. (11) and (12), we see that for the pure pion phase, $D(u) = 3Ba_1^A(u)$ and thus it must be large for the most range of u as well. In the multiquark configuration, the d dependence of $D(u_c)$ in the expression of F , Eqn. (12), will compensate the largeness of $D(u)$ and x'_4 can be made sufficiently large so that $L_0 = 1$ could still be satisfied. However, in pure pion phase, $D(u_c)$ is simply zero. This makes x'_4 getting smaller as the density gets larger and the scale fixing condition $L_0 = 1$ would not be satisfied above certain value of the density for a fixed B .

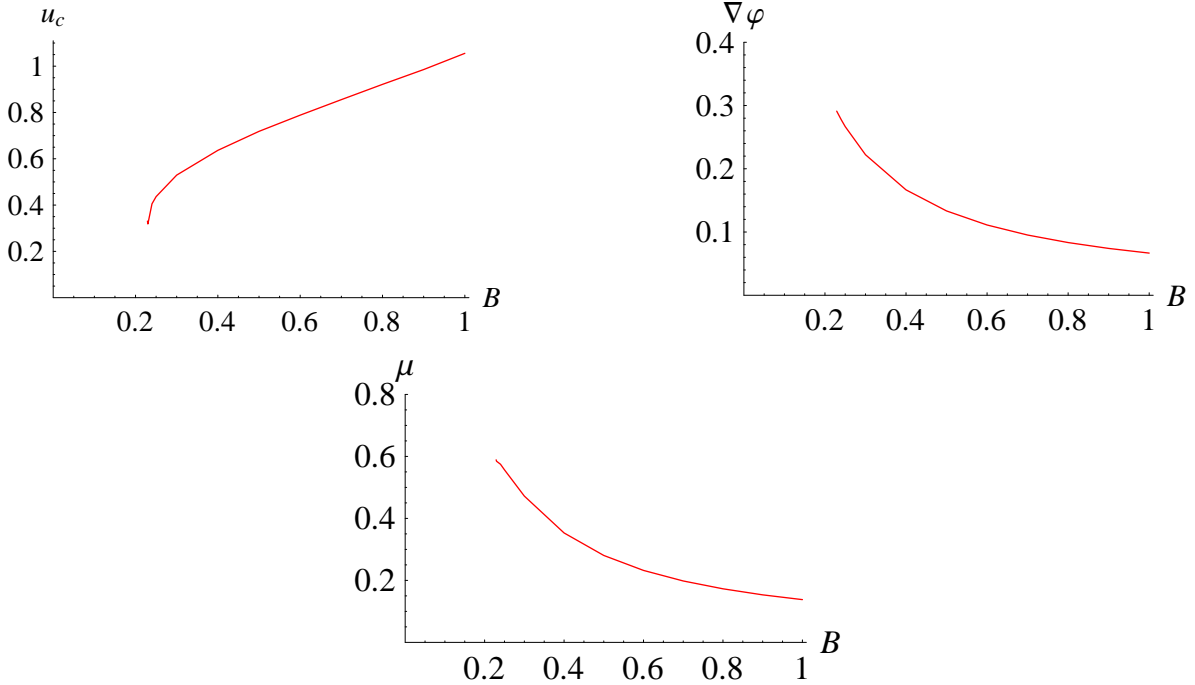


Figure 10: The position u_c , the pion gradient field, and the baryon chemical potential of the pure pion gradient phase at $d = 0.10, T = 0.10$ as a function of the magnetic field.

As a result, we wish to keep $\nabla\varphi$ sufficiently small in order to satisfy the scale fixing condition. This implies that higher densities require larger magnetic fields. To demonstrate this, we fix baryon density to $d = 0.1$ and plot the position u_c of the vertex and the baryon chemical potential as a function of the magnetic field in Fig. 10. The graph of u_c shows a minimal field at about $B \approx 0.229$ below which $L_0 < 1$ for all solutions. For a larger density $d \geq 1$, the required field strengths are $B \gg 1$ in order for the scale fixing condition to be satisfied. For the range of parameters $d = 1.0, B \leq 1.0$, we therefore need to consider only the two phases of the multiquark and the χ_S -QGP. The same situation occurs for the range of parameters $d = 10, B \leq 1 - 2$ where the pure pion gradient phase does NOT satisfy the scale fixing condition and therefore does not exist as well.

4.2 Multiquark-domain wall versus χ_S -QGP phase

The baryon chemical potential μ is to be found by shooting algorithm for a fixed d, B, T , for each phase. For $d = 1, B = 0.10, T = 0.10$, they are shown in Fig. 11. Observe that there are two possible solutions for the χ_S -QGP phase. As the magnetic field increases beyond a certain value (in this case around $B \approx 0.25$), there will be phase transition to another solution within this phase. This behaviour is explored in details in Ref. [19]. When the density is raised to $d = 10$, the transition occurs at higher field around $B \approx 0.86$ (Fig. 14). The transitions can also be seen in the plots of the free energy, Fig. 12,15, where the slopes of the graphs change abruptly around the critical fields. For $d = 1$, this is quite small and

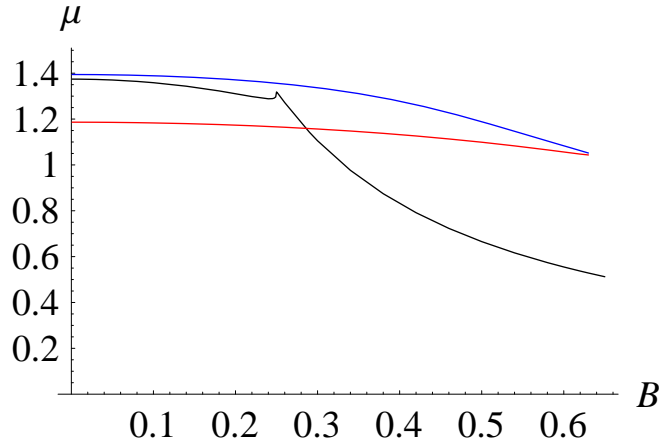


Figure 11: Comparison between the baryon chemical potential for $T = 0.10$ at a fixed density $d = 1$ of (a) $n_s = 0$ (normal baryon) multiquark configuration-**A**, the top (blue) graph,(b) χ_S -QGP, the middle (black) graph,(c) $n_s = 0$ (normal baryon) multiquark configuration-**B**, the bottom (red) graph.

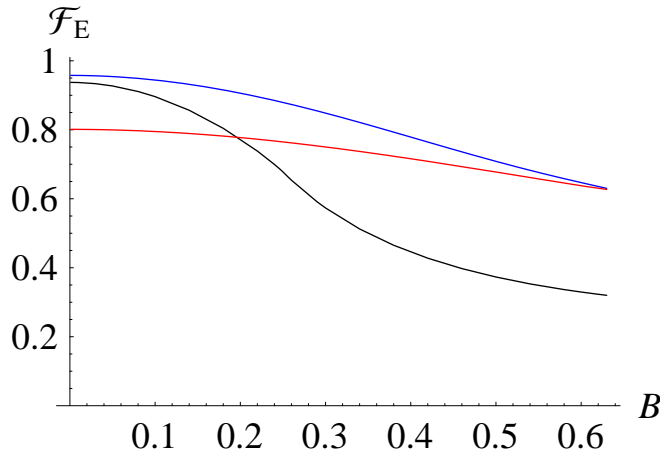


Figure 12: Comparison between the free energy for $T = 0.10$ at a fixed density $d = 1$ of (a) $n_s = 0$ (normal baryon) multiquark configuration-**A**, the top (blue) graph,(b) χ_S -QGP, the middle (black) graph,(c) $n_s = 0$ (normal baryon) multiquark configuration-**B**, the bottom (red) graph .

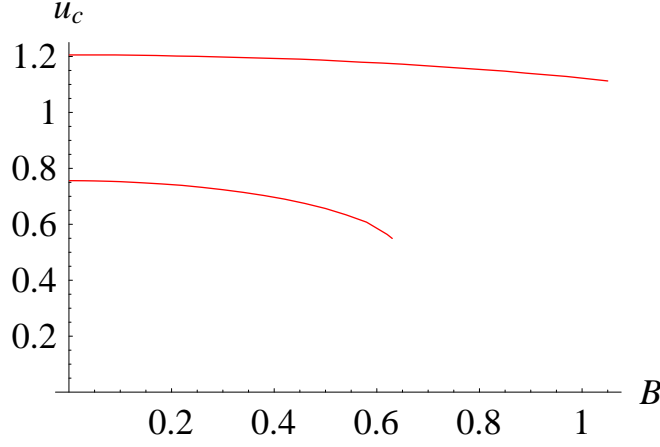


Figure 13: The position of the vertex u_c as a function of B at a fixed density $d = 1$ (lower) and $d = 10$ (upper) for $T = 0.10$ of $n_s = 0$ (normal baryon) multiquark configuration-**B** phase.

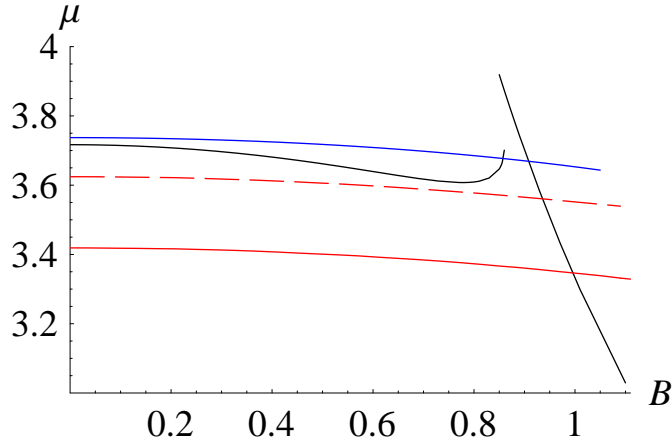


Figure 14: Comparison between the baryon chemical potential for $T = 0.10$ at a fixed density $d = 10$ of (a) $n_s = 0$ (normal baryon) multiquark configuration-**A**, the top (blue) curve,(b) χ_S -QGP, the black curve,(c) $n_s = 0.2$ multiquark configuration-**B**, the dashed red curve,(d) $n_s = 0$ (normal baryon) multiquark configuration-**B**, the red curve.

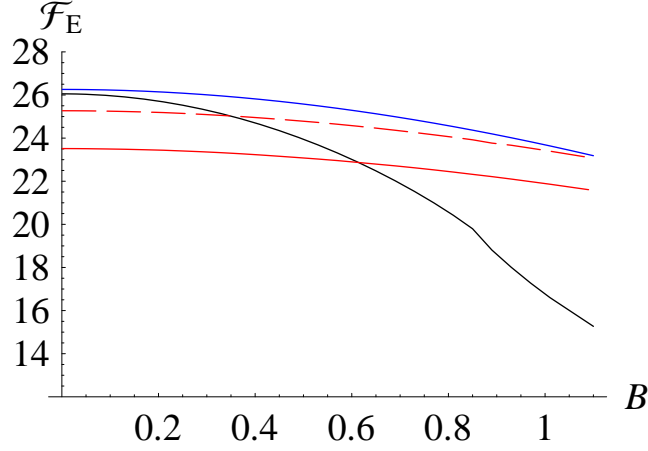


Figure 15: Comparison between the free energy for $T = 0.10$ at a fixed density $d = 10$ of (a) $n_s = 0$ (normal baryon) multiquark configuration-**A**, the top (blue) curve, (b) χ_S -QGP, the black curve, (c) $n_s = 0.2$ multiquark configuration-**B**, the dashed red curve, (d) $n_s = 0$ (normal baryon) multiquark configuration-**B**, the red curve.

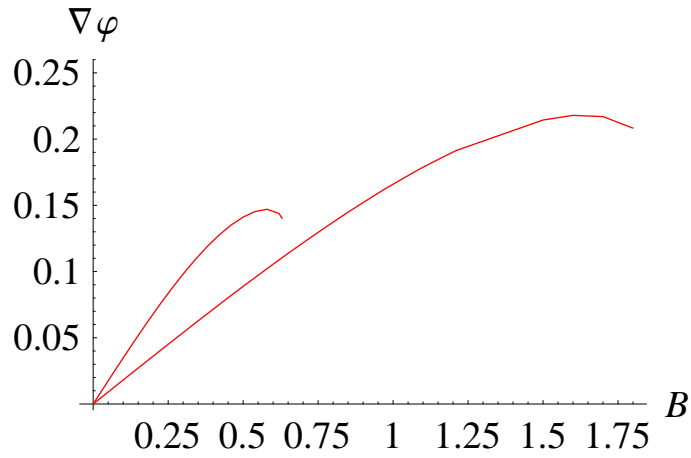


Figure 16: Plots between the pion gradient field of the multiquark phase and the magnetic field for $T = 0.10, n_s = 0$ at $d = 1$ (shorter) and $d = 10$ (longer).

somewhat hard to see but it becomes apparent for $d = 10$.

From the plots of the free energy, Fig. 12, the multiquark configuration-**A** is the least preferred phase when the density is small ($d = 1$). Its free energy is larger than the χ_S -QGP phase for all fields. For $B \leq 0.196$, the most preferred phase is the multiquark configuration-**B** phase with the lower free energy. The χ_S -QGP phase is more stable for $d = 1, B > 0.196$. Nevertheless, the multiquark configurations can exist up to only about the critical fields beyond which they cannot satisfy the scale fixing condition at that particular density.

However, this does not mean that the multiquarks phase cannot exist in the range of field larger than the critical value. Stronger field gives the D8-branes larger tension and thus it requires sufficiently heavier vertex and strings to pull it down in order for the distance between D8 and $\overline{D8}$ to reach $L_0 = 1$. This implies that we need larger d in order to make the configuration satisfy the scale fixing condition at stronger fields. Fig. 13,14,15 confirm this insight. They show the plots of the multiquarks configurations when the density is large ($d = 10$). Multiquark configurations can exist far beyond the critical field $B \approx 0.63$ of the small d case ($d = 1$). In particular, Fig. 15 demonstrates that at $d = 10$, the multiquark configurations ($n_s = 0, 0.2$), with lower free energies, are thermodynamically preferred over the χ_S -QGP for $B < 0.61$ and $B < 0.348$ respectively.

It is thus reasonable to conclude that for larger densities, the multiquarks phase will be more and more preferred over the χ_S -QGP phase, in a larger and larger range of the field. Magnetized multiquarks and the induced pion gradient field are thus stable thermodynamically and they will mix together in the magnetized nuclear (multiquark-domain wall) phase provided that the density is sufficiently large and the temperature is not too high.

Finally for completeness, we present the plots of the pion gradient field of the multi-quark phase (Fig. 16), the pion gradient field becomes smaller for a given B as the density increases. However, it extends to larger range of fields for larger density. We can therefore conclude that at the large densities (and baryon chemical potential), contribution of the pion gradient becomes lesser and the multiquarks contribute dominantly to the baryon density and chemical potential. This is also shown in Fig. 4.

5 Discussions and Conclusion

In Sakai-Sugimoto model, chiral symmetry restoration and gluon deconfinement are two distinct phase transitions. Generically, with an exception of the antipodal case with $x'_4 = 0$, gluon deconfinement occurs at lower temperature than the chiral symmetry restoration. For the region of the phase diagram between the two transitions, coloured multiquarks can exist with thermodynamical stability (the phase diagram is shown in Figure 8 of Ref.[7]).

Magnetic responses of the nuclear phase with colour multiquarks are studied here by using one component of the $U(1)$ subgroup of $U(N_f)$ as the vector potential of the external magnetic field. The Chern-Simon action of the D8-branes couples the magnetic field to an axial vector component, a_1^A , of the $U(1)$, inducing axial current j_A . When the chiral symmetry is broken, we effectively set j_A to zero. The value of $a_1^A(\infty)$ then describes the degree of chiral symmetry breaking of the phase.

There are two possible multiquark configurations **A** and **B**. Configuration-**A** is the configuration where the baryon vertex is close to the horizon. Configuration-**B**, on the other hand, has the baryon vertex more separated from the horizon. By comparing the free energy of the two configurations in Fig. 9, we found that configuration-**B** is more stable thermodynamically. We establish relations between the baryon chemical potential and the baryon density, the external magnetic field, and the temperature for both configurations as are shown in Fig. 3. Baryon chemical potential is an increasing function of the density when the field is turned on. This is the same behaviour to the case when there is no field.

On the other hand, the relation between chemical potential and the magnetic field is rather interesting. The baryon chemical potential is a decreasing function of the field. For multiquarks with high value of n_s (number of radial strings), the configuration finds it more difficult to satisfy the scale fixing condition at large fields. There is a maximum field strength for each n_s above which the multiquark configuration cannot exist (Fig. 6). This is in contrast to the behaviour of the chiral-symmetric quark-gluon plasma (in the antipodal case of the Sakai-Sugimoto model with no instantons, *i.e.* $x'_4(u) = 0$ case) studied in Ref. [16] where chemical potential is always a decreasing function with respect to B and the configuration continues to exist at arbitrarily large fields. This is due to the fixation of the density. Stronger field gives the flavour branes more tension and when the field is too strong, a fixed density source would not be sufficiently heavy to pull the branes down for the distance between D8 and $\overline{\text{D8}}$ to reach $L_0 = 1$. Temperature also has effect on the multiquarks, sufficiently high temperature will melt away the multiquarks even in the presence of an external field.

The gradient of the scalar field representing the chiral symmetry breaking, $\nabla\varphi = a_1^A(\infty)$, is found to roughly increase in magnitude with the field. For the same field strength and fixed density, multiquarks with higher n_s (*i.e.* larger colour charges) show higher degree of chiral symmetry breaking (larger magnitude of $a_1^A(\infty)$), but can only sustain the force condition up to smaller fields as is shown in Fig. 7.

The mixing of pion gradient with the multiquark in the multiquark phase decreases as the density increases (Fig. 4). It is found that the pure pion gradient phase (no multiquark contribution) does not satisfy the scale fixing condition for large densities and moderate fields.

What would happen if the magnetic field increases beyond the point where the multiquarks can satisfy the scale fixing condition $L_0 = 1$? We would expect the multiquarks to change into the multiquarks with lower n_s as is shown in Fig. 6 for a fixed d and T since they can still satisfy the scale fixing condition. This induces a sudden drop in the baryon chemical potential. Also in the situation where μ is kept fixed instead of d , the multiquarks are forced to jump to the larger d in order to change into the multiquarks with lower n_s as the field increases beyond the critical point. For even larger fields, all of the multiquarks cannot satisfy the scale fixing condition for a fixed density. There would be phase transition to other phase. For a fixed density, the phase will change into the χ_S -QGP. However, if we allow the density to change (in a more realistic situation), the system could change into the multiquark (with pion gradient mixing) phase for a sufficiently large density. The phase of multiquark with pion gradient mixing is found to be more preferred than the χ_S -QGP at large densities (implying large baryon chemical potentials) and moderate fields. This is

shown in Fig. 15.

For configuration-**B** multiquarks, The magnetization of the multiquark nuclear matter is found to be an increasing function of B for $n_s = 0, 0.10, 0.20$ except when the fields get close to the critical points. Close to the critical fields, the magnetizations saturate and even start to decrease. The magnetized multiquarks phases are thermodynamically preferred over the magnetized vacuum once the baryon chemical potential is higher than the onset value ($\mu > \mu_{onset}$). This is similar to the case when there is no magnetic field investigated in Ref. [7].

Acknowledgments

I would like to thank Ekapong Hirunsirisawat for help with the first illustration. P.B. is supported in part by the Thailand Research Fund (TRF) and Commission on Higher Education (CHE) under grant MRG5180227.

A Force condition of the multiquark configuration

The forces on the D4-brane in the flavour D8-branes are balanced among three forces from the tidal weight of the D4-brane, the force from the strings attached to the D4, and the force from the D8-branes. Varying the total action with respect to u_c gives the surface term. Together with the scale-fixing condition $2 \int_{u_c}^{\infty} dx'_4(u) = L_0 = 1$, we obtain [6]

$$x'_4(u_c) = \left(\tilde{L}(u_c) - \frac{\partial S_{source}}{\partial u_c} \right) \bigg/ \frac{\partial \tilde{S}}{\partial x'_4} \bigg|_{u_c}, \quad (16)$$

as the condition on u_c .

The Legendre transformed action is given by

$$\begin{aligned} \tilde{S} &= \int_{u_c}^{\infty} \tilde{L}(x'_4(u), d) du, \\ &= \mathcal{N} \int_{u_c}^{\infty} du \sqrt{\frac{1}{f(u)} + u^3 x_4'^2} \\ &\quad \times \sqrt{f(u)(C(u) + D(u)^2) - \left(j_A - \frac{3}{2} B \mu + 3 B a_0^V \right)^2}, \end{aligned} \quad (17)$$

where $C(u) \equiv u^5 + B^2 u^2$, $D(u) \equiv d + 3 B a_1^A(u) - 3 B \nabla \varphi / 2$. It is calculated by performing Legendre transformation with respect to $a_0^{V'}$ and $a_1^{A'}$ respectively. Note that the Chern-Simon action is also included in the total action during the transformations.

The Chern-Simon term with the derivatives $a^{V'}$, $a^{A'}$ eliminated is

$$S_{CS} = -\mathcal{N} \frac{3}{2} B \int_{u_c}^{\infty} du \frac{\left(a_0^V (j_A - \frac{3}{2} B \mu + 3 B a_0^V) - f(u) D(u) a_1^A \right) \sqrt{\frac{1}{f(u)} + u^3 x_4'^2}}{\sqrt{f(u)(C(u) + D(u)^2) - \left(j_A - \frac{3}{2} B \mu + 3 B a_0^V \right)^2}}. \quad (18)$$

Lastly, in order to compute $x'_4(u_c)$ we consider the source term [7]

$$S_{source} = \mathcal{N}d \left[\frac{1}{3}u_c \sqrt{f(u_c)} + n_s(u_c - u_T) \right], \quad (19)$$

$$= \mathcal{N}d\mu_{source} \quad (20)$$

where $n_s = k_r/N$ is the number of radial strings in the unit of $1/N$.

From Eqn. (16),(17),(18),(20), and setting $a_0^V(u_c) = \mu_{source}$, $a_1^A(u_c) = 0$ we can solve to obtain

$$(x'_4(u_c))^2 = \frac{1}{f_c u_c^3} \left[\frac{9}{d^2} \frac{(f_c(C_c + D_c^2) - (j_A - \frac{3}{2}B\mu + 3Ba_0^V(u_c))^2)}{(1 + \frac{1}{2}(\frac{u_T}{u_c})^3 + 3n_s\sqrt{f_c})^2} - 1 \right]$$

where $f_c \equiv f(u_c)$, $C_c \equiv C(u_c)$, $D_c \equiv D(u_c)$.

When we fix the parameter n_s , the temperature T , the baryon density d , the axial current $j_A = 0$ (by minimizing the action with respect to $a_1^A(\infty)$), and setting $a_1^A(u_c) = 0$, $a_0^V(u_c) = \mu_{source}$, then the position u_c of the D4-brane is completely determined as a function of the magnetic field B . Once the equations of motion are solved, the value of $\mu = a_0^V(\infty)$ and $a_1^A(\infty)$ are determined.

References

- [1] J. M. Maldacena, “The Large N Limit of Superconformal Field Theories and Supergravity,” *Adv. Theor. Math. Phys.* **2** (1998) 231-252 [*Int. J. Theor. Phys.* **38** (1999) 1113-1133], [arXiv:hep-th/9711200].
- [2] O. Aharony, S. S. Gubser, J. M. Maldacena, H. Ooguri, Y. Oz, “Large N Field Theories, String Theory and Gravity,” *Phys. Rept.* **323** (2000) 183-386, [arXiv:hep-th/9905111].
- [3] T. Sakai and S. Sugimoto, “Low Energy Hadron Physics in Holographic QCD,” *Prog. Theor. Phys.* **113** (2005) 843, [arXiv:hep-th/0412141].
- [4] T. Sakai and S. Sugimoto, “More on a Holographic Dual of QCD,” *Prog. Theor. Phys.* **114** (2005) 1083, [arXiv:hep-th/0507073].
- [5] O. Aharony, J. Sonnenschein and S. Yankielowicz, “A Holographic Model of Deconfinement and Chiral Symmetry Restoration,” *Annals Phys.* **322** (2007) 1420, [arXiv:hep-th/0604161].
- [6] Oren Bergman, Gilad Lifschytz, Matthew Lippert, “Holographic Nuclear Physics,” *JHEP* **11** (2007) 056, [arXiv:hep-th/0708.0326].
- [7] P. Burikham, A. Chatrabhuti, E. Hirunsirisawat, “Exotic multi-quark states in the deconfined phase from gravity dual models,” *JHEP* **05** (2009) 006, [arXiv:0811.0243, hep-ph].
- [8] A. Brandhuber, N. Itzhaki, J. Sonnenschein and S. Yankielowicz, “Baryon from supergravity,” *JHEP* **07** (1998) 046, [arXiv:hep-th/9806158].
- [9] O. Antipin, P. Burikham and J. Li, “Effective Quark Antiquark Potential in the Quark-Gluon Plasma from Gravity Dual Models,” *JHEP* **06** (2007) 046, [arXiv:hep-ph/0703105].
- [10] K. Ghoroku, M. Ishihara, A. Nakamura and F. Toyoda, “Multi-Quark Baryons and Color Screening at Finite Temperature,” *Phys. Rev.* **D79** (2009) 066009, [arXiv:0806.0195, hep-th].
- [11] K. Ghoroku and M. Ishihara, “Baryons with D5 Brane Vertex and k -Quarks States,” *Phys. Rev.* **D77** (2008) 086003, [arXiv:0801.4216, hep-th].
- [12] M.V. Carlucci, F. Giannuzzi, G. Nardulli, M. Pellicoro and S. Stramaglia, “AdS-QCD quark-antiquark potential, meson spectrum and tetraquarks,” *Eur. Phys. J.* **C57** (2008) 569, [arXiv:0711.2014, hep-ph].
- [13] W-Y. Wen, “Multi-quark potential from AdS/QCD,” *Int. J. Mod. Phys.* **A23** (2008) 4533, [arXiv:0708.2123, hep-th].

- [14] Oren Bergman, Gilad Lifschytz, Matthew Lippert, “Response of Holographic QCD to Electric and Magnetic Fields,” *JHEP* **05** (2008) 007, [arXiv:0802.3720, hep-th].
- [15] Clifford Johnson, Arnab Kundu, “External Fields and Chiral Symmetry Breaking in the Sakai-Sugimoto Model,” *JHEP* **12** (2008) 053, [arXiv:0803.0038, hep-th].
- [16] Oren Bergman, Gilad Lifschytz, Matthew Lippert, “Magnetic properties of densed Holographic QCD,” *Phys. Rev.* **D79** (2009) 105024, [arXiv:0806.0366, hep-th].
- [17] E.G. Thompson, D.T. Son, “Magnetized baryonic matter in holographic QCD,” *Phys. Rev.* **D78** (2008) 066007, [arXiv:0806.0367, hep-th].
- [18] Clifford Johnson, Arnab Kundu, “Meson Spectra and Magnetic Fields in the Sakai-Sugimoto Model,” *JHEP* **07** (2009) 103, [arXiv:0904.4320, hep-th].
- [19] Gilad Lifschytz, Matthew Lippert, “Holographic Magnetic Phase Transition,” [arXiv:0906.3892, hep-th].
- [20] E. Witten, “Baryons and Branes in Anti-de Sitter Space,” *JHEP* **07** (1998) 006, [arXiv:hep-th/9805112].
- [21] D. J. Gross and H. Ooguri, “Aspects of large N gauge theory dynamics as seen by string theory,” *Phys. Rev.* **D58** (1998) 106002, [arXiv:hep-th/9805129].
- [22] D. T. Son and M. A. Stephanov, *Phys. Rev.* **D77** (2008) 014021, [arXiv:0710.1084, hep-ph].